

Dynamic phase transition of ferroelectric nanotube described by a spin-1/2 transverse Ising model

Chundong Wang(王春栋), Ying Wu(吴瑛), Yulin Cao(曹喻霖), and Xinying Xue(薛新英)

Citation: Chin. Phys. B, 2021, 30 (**2**): 020504. DOI: 10.1088/1674-1056/abbbfd
Journal homepage: http://cpb.iphy.ac.cn; http://iopscience.iop.org/cpb

What follows is a list of articles you may be interested in

Entangled multi-knot lattice model of anyon current

Tieyan Si(司铁岩)
Chin. Phys. B, 2019, 28 (**4**): 040501. DOI: 10.1088/1674-1056/28/4/040501

Fidelity spectrum: A tool to probe the property of a quantum phase

Wing Chi Yu, Shi-Jian Gu
Chin. Phys. B, 2016, 25 (**3**): 030501. DOI: 10.1088/1674-1056/25/3/030501

Comment on 'Mathematical structure of the three-dimensional (3D)Ising model'

Jacques H. H. Perk
Chin. Phys. B, 2013, 22 (**8**): 080508. DOI: 10.1088/1674-1056/22/8/080508

Mathematical structure of the three-dimensional (3D) Ising model

Zhang Zhi-Dong
Chin. Phys. B, 2013, 22 (**3**): 030513. DOI: 10.1088/1674-1056/22/3/030513

Phase diagrams of spin-3/2 Ising model in the presence of random crystal field within the effective field theory based on two approximations

Ali Yigit, Erhan Albayrak
Chin. Phys. B, 2013, 22 (**10**): 100508. DOI: 10.1088/1674-1056/22/10/100508

Dynamic phase transition of ferroelectric nanotube described by a spin-1/2 transverse Ising model*

Chundong Wang(王春栋)[1,2], Ying Wu(吴瑛)[1,†], Yulin Cao(曹喻霖)[3,‡], and Xinying Xue(薛新英)[4,§]

[1] College of Life Science, Tarim University, Alaer 843300, China
[2] School of Optical and Electronic Information, Wuhan National Laboratory for Optoelectronics, Huazhong University of Science and Technology, Wuhan 430074, China
[3] Physics Laboratory, Industrial Training Center, Shenzhen Polytechnic, Shenzhen, China
[4] Department of Physics, College of Science, Shihezi University, Xinjiang 832003, China

(Received 26 July 2020; revised manuscript received 22 August 2020; accepted manuscript online 28 September 2020)

The dynamic phase transition properties for ferroelectric nanotube under a spin-1/2 transverse Ising model are studied under the effective field theory (EFT) with correlations. The temperature effects on the pseudo-spin systems are unveiled in three-dimensional (3-D) and two-dimensional (2-D) phase diagrams. Moreover, the dynamic behaviors of exchange interactions on the 3-D and 2-D phase transitions under high temperature are exhibited. The results present that it is hard to obtain pure ferroelectric phase under high temperature; that is, the vibration of orderly pseudo-spins cannot be eliminated completely.

Keywords: ferroelectric nanotube, three-dimensional (3-D) phase diagram, Ising model, dynamic phase transitions

PACS: 05.50.+q, 77.80.B− **DOI:** 10.1088/1674-1056/abbbfd

1. Introduction

Ferroelectrics have been recognized as one of the most promising functional materials as they are widely used in nonvolatile ferroelectric random access memories (FeRAM), micro-actuators, sensors, and micro-electro-mechanical systems (MEMS) because of their outstanding ferroelectric and piezoelectric performances.[1–3] Recently, high Curie temperature (T_C) materials, such as $BiScO_3$–$PbTiO_3$, $Bi(Zn_{1/2}$-$Ti_{1/2})O_3$–$PbTiO_3$ (BZT–PT), have been successfully fabricated.[4,5] Noteworthy, large remnant polarization with small leakage was realized in $Bi(Zn_{1/2}Zr_{1/2})O_3$–$PbTiO_3$.[6] Theoretically, transverse field and crystal field Ising model including different disorder distributions (dilution and randomness) has been widely adopt to understand the phase transition features of ferroelectrics. By using the standard linear response theory within the transfer matrix method, Chatterjee[7] studied the transverse susceptibility of spin-3/2 Ising chains under a crystal field. By applying the pair approximation within the discretized path integral representation, Wang *et al.*[8] investigated the critical properties of the Ising model under both random longitudinal and transverse fields. It is well acknowledged that the transverse Ising model (TIM) developed by Gennes *et al.*[9] (i.e., a pseudo-spin model of hydrogen-bonded ferroelectrics) should be more suitable to study the phase transition properties of the order–disorder type ferroelectric systems. Within the framework of mean-field approximation (MAF) under TIM, our group studied the inserting-layer effect, defect-layer effect, and seeding-layer effect in ferroelectric thin films, unveiling the phase transition features of the epitaxial ferroelectric films,[10–17] and presenting the spin-polarization of the ferroelectric supperlattice and crossover properties of the interaction parameters of the ferroelectric thin films. Using revised Fermi-type Green's function, Teng *et al.*[18] revealed the transition regions in the parameter space of ferroelectric thin film with four-spin interactions. By employing Green's function, Wesselinowa *et al.*[19–22] systematically studied the critical behaviors, dielectric phenomenon, and dynamic phase transition properties of the ferroelectric thin film and even nanoparticles within the TIM. Additionally, an effective-field theory (EFT) with correlations developed by Kaneyoshi[23,24] was also suggested to be an essential useful method for solving TIM. By comparison, it was found that FET is more precise than the mean-field theory (MFA) which is comparable to the Zernike approximation (ZA).[25] Numerous calculations of ferroelectric thin film, nanotube, nanowire, and nanoparticles were conducted by using FET so far, disclosing the dynamic phase transition behaviors of cylindrical ferroelectric nanotubes,[26] nanoscaled transverse

*Project supported by the National Key R&D Program of China (Grant No. 2017YFE0120500), the National Natural Science Foundation of China (Grant No. 51972129), the South Xinjiang Innovation and Development Program of Key Industries of Xinjiang Production and Construction Corps (Grant No. 2020DB002), the Fundamental Research Funds for the Central Universities, China (Grant Nos. HUST 2018KFYYXJJ051 and 2019KFYXMBZ076), and Shenzhen Fundamental Research Fund (Grant No. JCYJ20190813172609404). C.D.W. acknowledges the Hubei "Chu-Tian Young Scholar" Program.

†Corresponding author. E-mail: wuyingjuyuan@163.com
‡Corresponding author. E-mail: caoyulin@szpt.edu.cn
§Corresponding author. E-mail: yyingxx@163.com

© 2021 Chinese Physical Society and IOP Publishing Ltd

Ising thin films with diluted surfaces,[27] ferrimagnetism in a decorated Ising nanowire,[28,29] effects of surface dilution cylindrical transverse Ising ferrimagnetic nanotubes,[30] and compensation temperature in a cylindrical Ising nanowire (or nanotube).[31,32] To the best of our knowledge, the three-dimensional (3-D) phase transition and the dynamic phase behaviors of the ferroelectric nanotube under high temperature have not yet been reported.

In this work, the temperature effect on the phase transition properties of a ferroelectric nanotube was investigated with a spin-1/2 transverse Ising model. In addition, the 3-D phase transition behaviors under the influence of the external exchange interaction J_s at high temperature were demonstrated.

2. The model

A schematic diagram depicting the cross-section profile of a cylindrical ferroelectric nanotube is demonstrated in Fig. 1. Noteworthy, each site in the model is occupied by an Ising pesdo-spin. Different form most of the nanotubes investigated by Kaneyoshi *et al.*,[30,31] our model, taking three-layer nanotubes as an example, contains the inner-surface shell, the out-surface shell, and the bulk-layer. And each pesdo-spin connected to the two nearest pesdo-spins is along all directions. The Hamiltonian of the system described by the Ising model under a transverse field (TIM) can be expressed as follows:[10–31]

$$H = -\frac{1}{2}\sum_{\langle i,j\rangle} J_{i,j} S_i^Z S_j^Z - \sum_i \Omega_i S_i^x, \tag{1}$$

where Ω_i is the transverse field, S_k $(k = i, j)$ is the Ising spin operator with $S_k = \pm 1/2$ at sites i and j. J is the nearest-neighbor pesdo-spin pair interaction coupling constant of intralayer or the adjacent interlayers. $\sum_{\langle i,j\rangle}$ runs over only the nearest-neighbor sites. For simplicity, we choose the same value of the exchange interactions J_s in the two surfaces (inner-surface and outside-surface). For the bulk-layer, J_2 is the interaction, while the couples between different layers are set as J_1. In addition, the difference of the transverse field for the three layers is also considered, such as Ω_s for the two outside-surfaces, while Ω is the one for layers in the bulk.

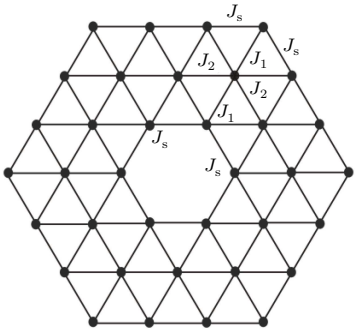


Fig. 1. Schematic diagram of a cylindrical nanotube.

Within the framework of the EFT,[23–26] the average value of pseudo-spins along the longitudinal direction (z-direction) in the i-th ($i = 1, 2, 3$) layer can be expressed as follows:

$$\begin{aligned} m_i &= \langle S_i^Z \rangle \\ &= \left\langle \prod_\delta \left[\cosh(J_{i,j+\delta}\nabla) + \xi_{j+\delta}\sinh(J_{i,j+\delta}\nabla)\right] \right\rangle f_i(x)\,|_{x=0}\,, \end{aligned} \tag{2}$$

where $\prod$ runs over only the nearest neighbors of site i, and z is the lattice coordination number, $\nabla = \partial/\partial x$ is the differential operator and one mathematical relation existing as follows:

$$\exp(\gamma\nabla) f(x) = (x + \gamma). \tag{3}$$

The function $f_\alpha(x)$ is defined as

$$f_\alpha(x) = \frac{x}{\sqrt{(2\Omega_\alpha)^2 + x^2}} \tanh\left(\frac{1}{4\beta}\sqrt{(2\Omega_\alpha)^2 + x^2}\right), \ (\alpha = \mathrm{s}, i), \tag{4}$$

where $\beta = \frac{1}{k_B T}$ (k_B is the Boltzmann constant), and T is the absolute temperature.

By employing Eq. (2), the longitudinal polarizations of each curved layer of the ferroelectric nanotube can be written as follows:

$$\begin{aligned} m_1 &= [\cosh(J_s\nabla) + m_1\sinh(J_s\nabla)]^4 \\ &\quad \times [\cosh(J_1\nabla) + m_2\sinh(J_1\nabla)]^3, \end{aligned} \tag{5}$$

$$\begin{aligned} m_2 &= [\cosh(J_2\nabla) + m_2\sinh(J_2\nabla)]^4 \\ &\quad \times [\cosh(J_1\nabla) + m_1\sinh(J_1\nabla)] \\ &\quad \times [\cosh(J_1\nabla) + m_3\sinh(J_1\nabla)]^3, \\ m_3 &= [\cosh(J_s\nabla) + m_3\sinh(J_s\nabla)]^4 \\ &\quad \times [\cosh(J_1\nabla) + m_2\sinh(J_1\nabla)]. \end{aligned} \tag{6}$$

Based on Eqs. (5) and (6), the following simple matrix can be obtained by neglecting the nonlinear terms:

$$\begin{vmatrix} 4A-1 & 3B & \\ C & 4D-1 & 3C \\ & E & 4F-1 \end{vmatrix} = 0, \tag{7}$$

with

$$A = \cosh^3(J_s\nabla)\sinh(J_s\nabla)\cosh^3(J_1\nabla), \tag{8}$$

$$B = \sinh(J_1\nabla)\cosh^2(J_1\nabla)\cosh^4(J_s\nabla), \tag{9}$$

$$C = \sinh(J_1\nabla)\cosh^3(J_1\nabla)\cosh^4(J_s\nabla), \tag{10}$$

$$D = \cosh^3(J_2\nabla)\sinh(J_2\nabla)\cosh^4(J_1\nabla), \tag{11}$$

$$E = \sinh(J_1\nabla)\cosh^4(J_s\nabla), \tag{12}$$

$$F = \sinh(J_s\nabla)\cosh(J_1\nabla)\cosh^3(J_s). \tag{13}$$

3. Numerical results and discussion

For distinguishing the outer and inside layers, we have three different exchange interactions J_s, J_1, and J_2, and two different transversal fields Ω_s and Ω_b for the outside-layer and the bulk layer, respectively. With these definitions, it allows us

to express the vivid dynamic phase transition features in three dimensions (i.e., R/J vs. Ω_s/J, Ω_b/J). It is noteworthy that R is used to stand for J_1 and all the results are in numerical discussion by covering a reduced arbitrary parameter J.

As is well known, temperature changes will lead to phase transition from ferroelectric (orderly state) to paraelectric (disorderly state), which has been widely observed in 2-D phase diagrams.[10–15] However, there are few 3-D phase diagrams showing the vivid phase transition of ferroelectrics up to now. Figure 2 exhibits the whole dynamic processes of the phase transition under the influence of temperature in three dimensions. In order to depict more details, the projections of the 3-D curve-surface are also demonstrated in Fig. 3 in sequences. Figure 2(a) shows a regular curve-surface with four up-foots touched the four vertexes nearly, indicating a regular ferroelectric phase. In its 2-D projection (Fig. 3(a)), it presents as concentric several regular ovals. When the temperature rises to 28.8, some vibration should be introduced in the ferroelectric phase, for which a bent rectangle along one axis is discerned as shown in Fig. 2(b). As expected, the two 2-D projection phase diagrams are also changed, showing as paralleled lines (Fig. 3(b)). With the temperature further increased to 30, the bent rectangle further sinks along backbone (another axis) as shown in Fig. 2(c). In this case, a squeezed curve is observed in a 2-D projection (Fig. 3(c)). As the temperature further increases to 80, the 3-D curve is more squeezed toward the backbone (Fig. 2(d)), and more densely curves are identified in its 2-D projection (Fig. 3(d)), suggesting that huge irregular states (paraelectric) have been caused in the ferroelectric systems with the temperature increasing. When the temperature is increased to 120, intensive vibration occurs on the surface of the 3-D bent curve (Fig. 2(e)), the variation behavior of which can also be reflected in the 2-D projection (Fig. 3(e)), indicating that more disorderly state has been developed to a considerable extent. Further increase the temperature to 180, the phase transition from ferroelectric to paraelectric is revealed as a random distribution in Fig. 2(e) and the zigzag curve in 2-D projection (Fig. 3(f)).

The phase transition behaviors from ferroelectric to paraelectric have been widely demonstrated in the previous works.[12–16] However, the 3-D phase transition behaviors under high temperature have seldom been reported. Figure 4(a) exhibits the paraelectric phase showing random distribution in 3-D curves (Ω_s/J vs. Ω_b/J; Fig. 4(a)) under $T = 100$ and $J_s = 0.3$. Similar to Fig. 3(f), the 2-D projection also presents a zigzag curve. When J_s is increased to 1, the surface vibrates and is highly squeezed, showing a bent rectangle shape (Fig. 4(b). In the 2-D projection shown in Fig. 5(b), squeezed curves can be observed accompanied with a faint vibration, indicating that some regular pesdo-spin system has been introduced. With J_s further increased to 6, less bent rectangle along backbone is observed, in which it can be observed that the surface is much smooth than the counterpart of small J_s (Fig. 4(c)). The corresponding 2-D projection presents more densely squeezed curves (Fig. 5(c)). This observation could be ascribed to the fact that the pesdo-spin systems are changing toward an orderly state. Further increasing J_s to 6.5 (Fig. 4(b)), as expected, a bent rectangle along one axis is observed similar to Fig. 2(b), which suggests that the system tends to be ferroelectric. The only difference between Fig. 2(b) and Fig. 4(d) is the vibration on the surface, which could be attributed to the fact that the investigated

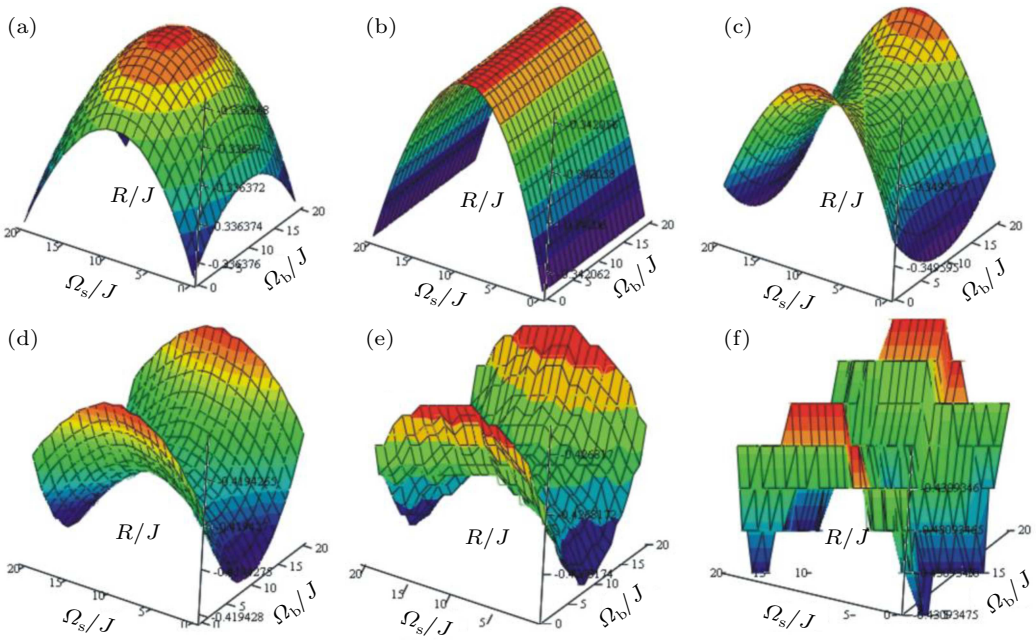


Fig. 2. Temperature induced 3-D phase diagrams (i.e. R/J vs. Ω_s/J, Ω_b/J) with $J_s = 2$, $J_2 = 2$: (a) $T = 28$, (b) $T = 28.8$, (c) $T = 30$, (d) $T = 80$, (e) $T = 120$, (f) $T = 180$.

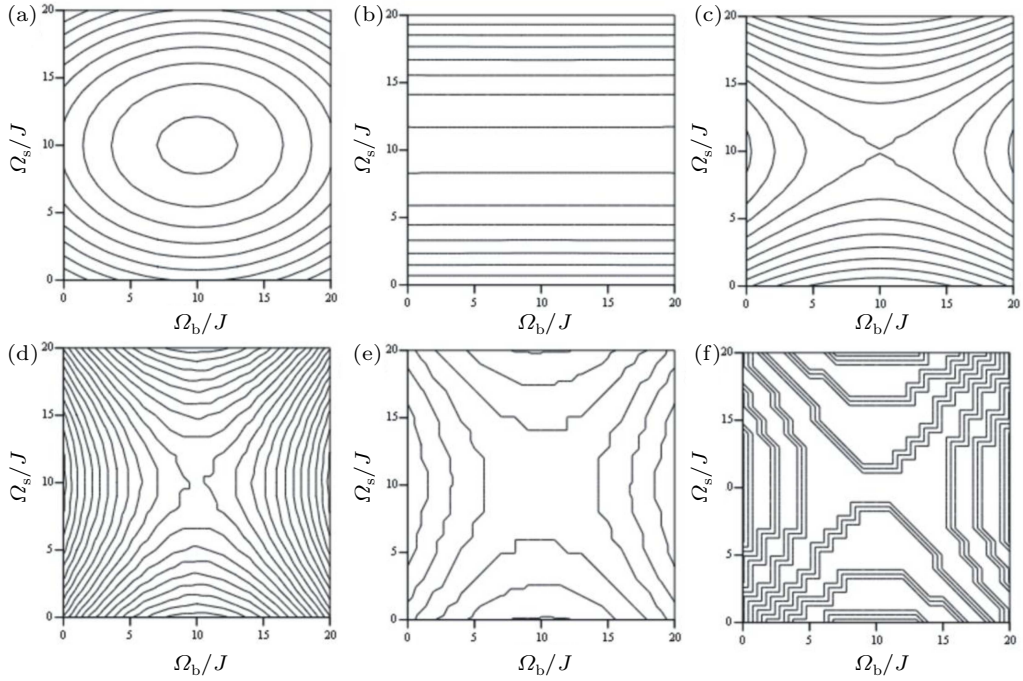


Fig. 3. The projection of 3-D curve-surface in 2-D plane (Ω_s/J vs. Ω_b/J).

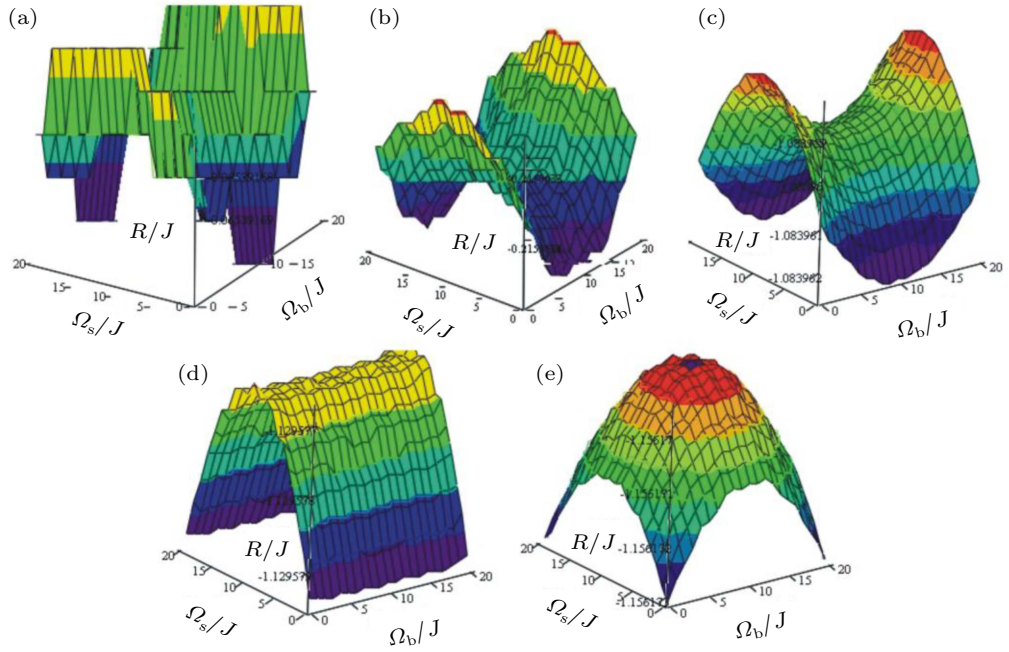


Fig. 4. The 3-D phase transition behaviors (i.e., R/J vs. Ω_s/J , Ω_b/J) under the influence of the external exchange interaction J_s at high temperature with $J_2 = 2$, $T = 100$: (a) $J_s = 0.3$, (b) $J_s = 1$, (c) $J_s = 6$, (d) $J_s = 6.5$, (e) $J_s = 6.9048$.

ferroelectric systems are under the high temperature $T = 100$. In the 2-D projection exhibited in Fig. 5(d), wavy lines array is observed. Finally, when J_s is increased to 6.9048, a regular curve-surface with four up-foots touches the four vertexes nearly, informing a ferroelectric phase has been obtained. It should be noted that the surface is still rough compared to the one shown in Fig. 2(a), the reason of which should be attributed to the fact that it is at relative high temperature, at which some paraelectric phase in the pseudo-spin polarizations system still exists. The observations are similarly in the corresponding 2-D projection, in which some faint vibrations are also revealed in the concentric circles (Fig. 5(e)). In the whole process of phase transition from the paraelectric to the ferroelectric, it is interesting to find that the vibrations of the pseudo-spins always exist even when the external exchange interaction is increased to enough large, suggesting that no matter how large the exchange interaction it is, it rarely has chance to change the system to perfect ferroelectric phase at high temperature.

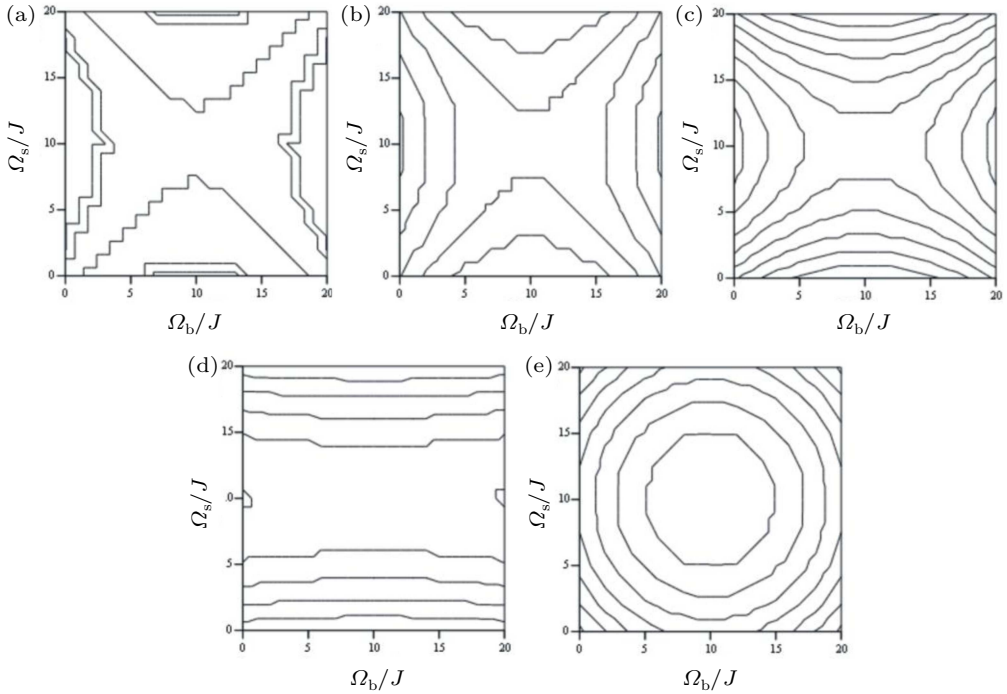


Fig. 5. The projection of J_s induced 3-D phase transition at high temperature in 2-D plane (Ω_s/J vs. Ω_b/J).

4. Conclusion

In summary, three-dimensional dynamic phase transition of ferroelectric nanotube in a spin-1/2 transverse Ising model has been examined using effective field theory. The temperature effects on phase transitions have been revealed both in 3-D and 2-D phase diagrams, demonstrating temperature to be the most important factor in guiding the phase. More interestingly, the phase transition behaviors under high temperature were investigated, informing that it always contains some paraelectric component in the ferroelectric phase even at large exchange interaction under high temperature. The 3-D phase transition behaviors under high temperature were studied for the first time.

References

[1] Scott J F and Dearaujo C A P 1989 *Science* **246** 1400
[2] Dearaujo C A P, Cuchiaro J D and McMillan L D 1995 *Nature* **374** 627
[3] Vrejoiu I, Alexe M and Hesse D 2008 *Adv. Funct. Mater.* **18** 3892
[4] Zhang X D, Kwon D and Kim B G 2008 *Appl. Phys. Lett.* **92** 082906
[5] Suchomel M R and Davies P K 2005 *Appl. Phys. Lett.* **86** 262905
[6] Zhang L, Chen J and Zhao H 2013 *Dalton Trans.* **42** 585
[7] Chatterjee I 1985 *J. Phys. C* **18** L1097
[8] Wang Y Q and Li Z Y 1994 *J. Phys.: Condens. Matter* **6** 10067
[9] de Gennes P G 1963 *Solid State Commun.* **6** 132
[10] Wang C D, Teng B H and Zhang X J 2008 *Mod. Phys. Lett.* **22** 3099
[11] Wang C D, Teng B H and Zhang X J 2009 *Physica A* **388** 1472
[12] Wang C D, Teng B H and Lu Z Z 2011 *Commun. Theor. Phys.* **55** 1024
[13] Wang C D, Teng B H and Kwok S Y 2011 *Commun. Theor. Phys.* **56** 1057
[14] Wang C D, Teng B H and Teng Y F 2010 *Commun. Theor. Phys.* **54** 756
[15] Lu Z X, Teng B H and Lu X H 2009 *Solid State Commun.* **149** 1176
[16] Wang B, Huang H L, Sun Z Y and Kou S P 2012 *Chin. Phys. Lett.* **29** 120301
[17] Meng Q K, Feng D T, Gao X T and Mei Y X 2012 *Chin. Phys. Lett.* **29** 120502
[18] Teng B H and Sy H K 2005 *Europhys. Lett.* **72** 823
[19] Michael Th, Trimper S and Wesselinowa J M 2007 *Phys. Rev. B* **76** 094107
[20] Wesselinowa J M 2002 *Solid State Comm.* **121** 489
[21] Wesselinowa J M and Trimper S 2002 *Int. J. Mod. Phys. B* **16** 473
[22] Wesselinowa J M 2002 *Phys. Status Solidi B* **231** 187
[23] Kaneyoshi T 2003 *J. Magn. Magn. Mater.* **264** 30
[24] Kaneyoshi T 2003 *Phys. Status Solidi B* **237** 592
[25] Kaneyoshi T 2003 *Physica A* **319** 355
[26] Wang C D, Lu Z Z, Yuan W X, Kwok S Y and Teng B H 2011 *Phys. Lett. A* **375** 3405
[27] Kaneyoshi T 2012 *Physica B* **407** 4358
[28] Kaneyoshi T 2012 *Phys. Lett. A* **376** 2352
[29] Divyamani B G and Sudha 2013 *Chin. Phys. Lett.* **30** 120301
[30] Kaneyoshi T 2011 *Solid State Commun.* **151** 1528
[31] Kaneyoshi T 2011 *Physica A* **390** 3697
[32] Zhang Q Y, Sun D K, Zhang and Y F and Zhu M F 2016 *Chin. Phys. B* **25** 066401